J. Chem. Eng. Data **2010,** *55,* 3262–3267

Extraction Ability of Nitrogen-Containing Compounds Involved in the Desulfurization of Fuels by Using Ionic Liquids

Luisa Alonso, Alberto Arce,* María Francisco, and Ana Soto

Department of Chemical Engineering, University of Santiago de Compostela, E-15782 Santiago de Compostela, Spain

---

In this work, the ability of some ionic liquids ($[C_8mim][BF_4]$, $[C_8mim][NTf_2]$, and $[C_2mim][EtSO_4]$), which have shown to be suitable as extraction solvents for the desulfurization of fuel oils, has been tested to carry out simultaneous denitrogenation. For this purpose, the liquid−liquid equilibria of these ionic liquids with pyridine and *n*-hexane have been determined at 298.15 K and atmospheric pressure. With the idea of giving useful parameters for the design of extraction units, the simultaneous correlation of five ternary systems involved in the gasoline and diesel desulfurization was carried out with the nonrandom two-liquid (NRTL) equation. The best results were achieved for a value of the nonrandomness parameter $\alpha = 0.3$.

---

1. Introduction

Petroleum is being depleted rapidly. The demand of sweet crude exceeds the world supply, and necessity is replacing sweet with heavy and sour crude. These terms refer to crude oils with more heavy components and with high sulfur content. Nonetheless, regulations regarding liquid hydrocarbon fuels are continuously requiring sulfur content to be reduced to lower levels. The current specification in Europe requires $10 \cdot 10^{-6}$, both for gasoline and diesel, and the tendency goes to sulfur-free fuel oils.

Because of the trend in supplying crude oil with heavier and higher sulfur content for refining and stronger environmental requirements, the problem of desulfurization has become of great importance. To achieve required desulfurization using the current hydrodesulfurization (HDS) technology, in most of the cases a two-stage deep desulfurization process is required; this also implies an increase of hydrogen rate, higher temperature, higher pressure, and more active catalysts. These alternatives are costly to refiners.

To solve all of these shortcomings of the HDS process, many research communities and refineries have pointed their efforts into the development of new approaches. Among them, ionic liquid (IL) extraction is one of the most attractive. ILs are defining the substitution of the organic solvents in traditional reaction and separation systems and the basis of several new processes.[1,2] These salts with melting temperatures below 100 °C could play an important role in desulfurization.

We have undertaken a systematic study[3−11] about the desulfurization of fuel oils by using the 1-octyl-3-methylimidazolium tetrafluoroborate, $[C_8mim][BF_4]$, 1-octyl-3-methylimidazolium bis(trifluoromethylsulfonyl)-imide, $[C_8mim][NTf_2]$, and 1-ethyl-3-methylimidazolium ethylsulfate, $[C_2mim][EtSO_4]$, ILs. Because an HDS process implies more reactions than desulfurization, we seek to close previous work by analyzing the ability of these ILs not only to desulfurizate but also to denitrogenate. For this reason, liquid−liquid equilibria (LLE) of several ternary systems involving *n*-hexane, pyridine, and the ILs are obtained experimentally. The LLE data are correlated by means of the nonrandom two-liquid (NRTL) equation.[12] Following this, the simultaneous correlations of the ternary LLE involved in the desulfurization and denitrogenation of gasoline and diesel fuels are carried out, with the aim of obtaining the interaction parameters required in the design and simulation of extraction columns where the industrial processes would take place.

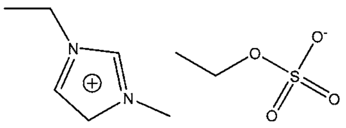

1-ethyl-3-methylimidazolium ethylsulfate

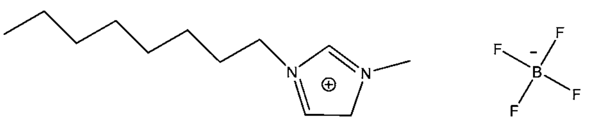

1-octyl-3-methylimidazolium tetrafluoroborate

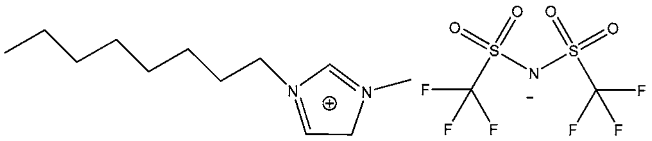

1-octyl-3-methylimidazolium bis{(trifluoromethyl)sulfonyl}imide

Figure 1. Chemical structure of the ILs.

2. Experimental Section

2.1. Chemicals. *n*-Hexane (Fluka, puriss. p.a. ACS $\omega \geq 0.990$), and pyridine (Riedel-de Häen, puriss. $\omega \geq 0.995$, GC) were used as received from the supplier without further purification. Gas chromatography (GC) analysis did not detect any appreciable peak of impurities.

---

* Corresponding author. Tel.: +34981563100 ext. 16790. Fax: +34981528050. E-mail address: alberto.arce@usc.es.

10.1021/je100075m

Table 1. Water Content ω_{H_20}, Density ρ, and Refractive Index n_D of the Pure Components at 298.15 K and Atmospheric Pressure

component	CAS Registry No.	$\omega_{H_20}\cdot10^{-6}$	ρ/g·cm^{-3} exptl	ρ/g·cm^{-3} lit.	n_D exptl	n_D lit.
n-hexane	110-54-3	75	0.65506	0.65484[13]	1.37287	1.37226[13]
pyridine	110-86-1	177	0.97802	0.97824[13]	1.50699	1.50745[13]
$[C_8mim][BF_4]$	244193-52-0	51	1.10442	1.103506[14]	1.43329	1.4322[15]
$[C_8mim][NTf_2]$	178631-04-4	21	1.31978	1.31[16]	1.43270	not found
$[C_2mim][EtSO_4]$	342573-75-5	148	1.23817	1.23763[17]	1.47903	1.47940[17]

The ILs used in this work were synthesized in our laboratory. 1-Methylimidazole was mixed with an excess of 1-chloro-octane to produce $[C_8mim][Cl]$. This chloride was mixed with $Li[NTf_2]$ or $Na[BF_4]$ salts, using deionized water as a solvent, thus obtaining the $[C_8min][NTf_2]$ or the $[C_8min][BF_4]$ by ion methathesis in a similar manner to that reported in previous papers.[3,5] The IL $[C_2mim][EtSO_4]$ was synthesized by direct reaction of equimolecular quantities of 1-methylimidazole (Aldrich, $\omega \geq 0.99$, GC) and 1-ethoxysulfonyloxyethane (Aldrich, $\omega > 0.98$, GC) in toluene. More details about the method of production can be found in a previous paper.[10] The synthesized ILs were analyzed by ^{1}H and ^{13}C NMR to confirm the absence of any major impurities. Estimated purity is $\omega > 0.995$ in all cases. The chemical structures of these ILs are represented in Figure 1.

In Table 1, the experimental densities, refractive indices, and water contents of the pure components used in this work are compared with the values published by other authors.[13−17]

2.2. Procedure. Experimental values for densities were obtained with viscosity correction in an Anton Paar DMA 5000 densimeter with an uncertainty in the measurement of $\pm\ 10^{-5}$ g·cm^{-3}. Refractive indices were measured in an Atago RX-5000 refractometer connected to a Heto Therm thermostat to keep constant temperature. The uncertainty in the refractive index measurement is $\pm\ 4\cdot10^{-5}$. The Karl Fischer titration method using a Metrohm 737 KF coulometer and Hydranal reagent (Riedel-de Haën) was employed for water content measurement. Weighing was carried out in a Mettler Toledo AT 261 balance, precise to within $\pm\ 10^{-4}$ g.

LLE data for ternary systems were determined experimentally by an analysis of the phases at equilibrium. To obtain the tie-lines, mixtures with compositions inside the immiscible region of the systems were introduced into 30 mL glass-jacketed vessels, with magnetic stirrers, and closed. The jackets were connected to a thermostat bath (Julabo F12) to maintain a constant temperature of 298.15 K in the vessels. Good contact between system components was guaranteed through 12 h of stirring (to completely reach the thermodynamic state) and 12 h to allow phases to settle down. Samples of both layers were withdrawn using syringes connected to long stainless steel needles. The composition of these equilibrium phases was analyzed by GC. Hexane and pyridine molar fractions were determined using an internal standard method, and IL composition was established by difference. The gas chromatograph used was an HP 6890 series equipped with a flame ionization detector (FID), a capillary column, and an empty precolumn to protect the column and collect the IL that could not be retained by the liner. The carrier gas used was helium, and the GC was equipped with an Autosampler 7683 series. Each sample was injected in quintuple to improve accuracy. The estimated uncertainty in the determination of mole fraction compositions is ± 0.006 for equilibrium data of studied ternary systems.The GC operating conditions are given in Table 2.

Table 2. Chromatographic Conditions for Composition Analysis

column	SPB-1 sulfur (30 m × 0.32 mm × 4 μm)	
detector type	FID	
detector temperature	523.15 K	
carrier gas	helium	split ratio 50:1
injector temperature	548.15 K	injection 1 μL
flow rate	2 mL·min^{-1}	
column oven	423.15 K, 5.5 min isothermal	

Table 3. Compositions of Experimental Tie-Lines, Solute Distribution Ratios (β), and Selectivities (S) for $[C_8mim][BF_4]$ (1) + Pyridine (2) + *n*-Hexane (3) at 298.15 K

IL-rich phase			hydrocarbon-rich phase				
x_1^{II}	x_2^{II}	x_3^{II}	x_1^{I}	x_2^{I}	x_3^{I}	β	S
0.855	0.000	0.145	0.003	0.000	0.997		
0.703	0.181	0.117	0.001	0.028	0.971	6.46	53.65
0.599	0.300	0.101	0.005	0.058	0.937	5.20	48.25
0.510	0.387	0.103	0.002	0.079	0.920	4.92	44.01
0.404	0.499	0.098	0.004	0.121	0.875	4.11	36.80
0.296	0.602	0.102	0.000	0.188	0.812	3.21	25.51
0.186	0.694	0.120	0.000	0.334	0.666	2.08	11.48
0.088	0.720	0.192	0.000	0.532	0.468	1.35	3.30

Table 4. Compositions of Experimental Tie-Lines, Solute Distribution Ratios (β), and Selectivities (S) for $[C_8mim][NTf_2]$ (1) + Pyridine (2) + *n*-Hexane (3) at 298.15 K

IL-rich phase			hydrocarbon-rich phase				
x_1^{II}	x_2^{II}	x_3^{II}	x_1^{I}	x_2^{I}	x_3^{I}	β	S
0.711	0.000	0.289	0.000	0.000	1.000		
0.597	0.160	0.243	0.006	0.018	0.977	9.14	36.77
0.500	0.276	0.225	0.000	0.047	0.953	5.89	24.96
0.408	0.381	0.211	0.004	0.061	0.934	6.23	27.53
0.353	0.442	0.205	0.006	0.080	0.914	5.51	24.53
0.278	0.520	0.203	0.005	0.119	0.876	4.37	18.88
0.213	0.584	0.203	0.003	0.149	0.848	3.92	16.41
0.126	0.635	0.239	0.004	0.297	0.699	2.14	6.26
0.066	0.642	0.292	0.001	0.425	0.574	1.51	2.97

Table 5. Compositions of Experimental Tie-Lines, Solute Distribution Ratios (β), and Selectivities (S) for $[C_2mim][EtSO_4]$ (1) + Pyridine (2) + *n*-Hexane (3) at 298.15 K

IL-rich phase			hydrocarbon-rich phase				
x_1^{II}	x_2^{II}	x_3^{II}	x_1^{I}	x_2^{I}	x_3^{I}	β	S
0.993	0.000	0.007	0.000	0.000	1.000		
0.869	0.123	0.008	0.002	0.048	0.951	2.58	316.25
0.705	0.286	0.009	0.000	0.094	0.906	3.02	293.96
0.540	0.447	0.013	0.000	0.206	0.794	2.17	130.66
0.395	0.586	0.019	0.000	0.341	0.659	1.72	58.86
0.320	0.657	0.023	0.000	0.515	0.485	1.28	27.02
0.248	0.725	0.028	0.000	0.625	0.375	1.16	15.81
0.168	0.786	0.045	0.000	0.771	0.229	1.02	5.17

3. Results and Discussion

3.1. Experimental LLE Data. The LLE data for the $[C_8min][BF_4]$ + pyridine + *n*-hexane, $[C_8mim][NTf_2]$ + pyridine + *n*-hexane, and $[C_2mim][EtSO_4]$ + pyridine + *n*-hexane ternary systems are reported in Tables 3 to 5. Also, in these tables values of the solute distribution ratio (β) and selectivity (S) can be seen, defined by following equations:

$$\beta = \frac{x_2^{\mathrm{II}}}{x_2^{\mathrm{I}}} \tag{1}$$

$$S = \frac{x_2^{\mathrm{II}} \cdot x_1^{\mathrm{I}}}{x_2^{\mathrm{I}} \cdot x_1^{\mathrm{II}}} \tag{2}$$

where x represents the mole fraction, subscripts 1 and 2 refer to inert (hexane) and solute (pyridine), and superscripts I and II refer to inert-rich phase and IL-rich phase, respectively.

Equilateral triangular diagrams with the graphical representation of the ternary LLE are shown in Figures 2 to 4. As can be seen, all studied ternary systems correspond to the type 1 category, with one of their constituent pairs exhibiting partial immiscibility and with only one immiscibility region. In all of these three systems the tie-line slopes show positive values.

3.1.1. Correlation of Experimental Ternary LLE Data. The correlation of the experimental data was done with the NRTL[12] equation. The value of the nonrandomness parameter, α, was previously assigned to 0.1, 0.2, and 0.3. The binary interaction parameters were obtained using a computer program developed by Sørensen and Arlt,[18] which uses two objective functions. First, F_a does not require any previous guess for parameters, and after convergence these parameters are used in the second function, F_b, to fit the experimental concentrations:

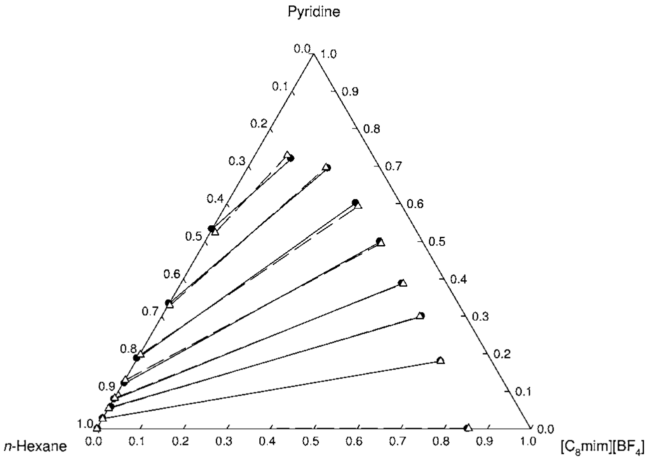

Figure 2. LLE for the ternary system [C$_8$mim][BF$_4$] (1) + pyridine (2) + *n*-hexane (3) at 298.15 K. Compositions of experimental tie-lines: ●, solid line; tie-lines correlated by NRTL equation: △, long dash.

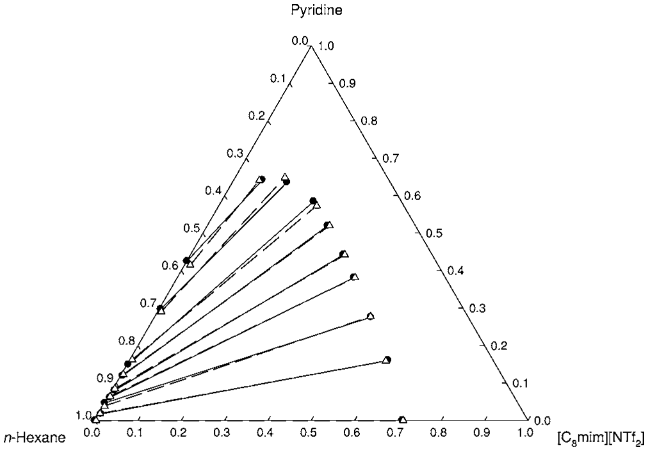

Figure 3. LLE for the ternary system [C$_8$mim][NTf$_2$] (1) + pyridine (2) + *n*-hexane (3) at 298.15 K. Compositions of experimental tie-lines: ●, solid line; tie-lines correlated by NRTL equation: △, long dash.

$$F_{\mathrm{a}} = \sum_k \sum_i [(a_{ik}^{\mathrm{I}} - a_{ik}^{\mathrm{II}})/(a_{ik}^{\mathrm{I}} + a_{ik}^{\mathrm{II}})]^2 + Q\sum_n P_n^{\ 2} \tag{3}$$

$$F_{\mathrm{b}} = \sum_k \mathrm{mim} \sum_i \sum_j (x_{ijk} - \hat{x}_{ijk})^2 + Q\sum P_n^{\ 2} + \left[\ln\left(\frac{\hat{\gamma}_{\mathrm{S}\infty}^{\mathrm{I}}}{\hat{\gamma}_{\mathrm{S}\infty}^{\mathrm{II}}}\beta_\infty\right)\right]^2 \tag{4}$$

where a is the activity, x is the experimental composition in mole fraction, and $\hat{x}$ the corresponding calculated composi-

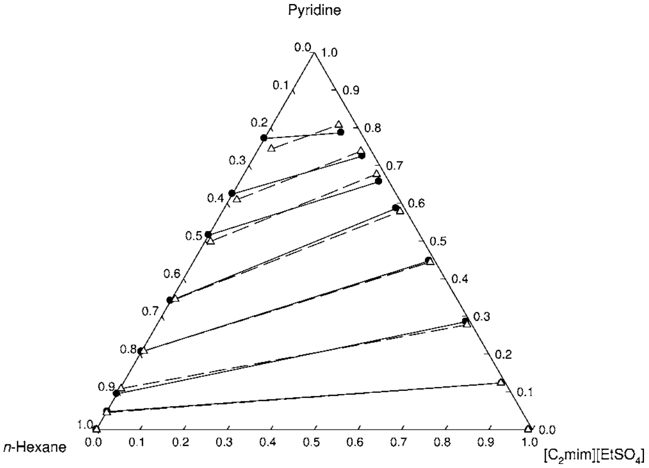

Figure 4. LLE for the ternary system [C$_2$mim][EtSO$_4$] (1) + pyridine (2) + *n*-hexane (3) at 298.15 K. Compositions of experimental tie-lines: ●, solid line; tie-lines correlated by NRTL equation: △, long dash.

Table 6. Binary Interaction Parameters and Root-Mean-Square Deviations (rmsd's) for the NRTL Correlation, without Fixing the Solute-Distribution Ratio at Infinite Dilution, of the Ternary Systems at 298.15 K

			components	parameters	
model	rmsd		$i-j$	Δg_{ij}/J·mol^{-1}	Δg_{ji}/J·mol^{-1}
[C$_8$mim][BF$_4$] (1) + Pyridine (2) + *n*-Hexane (3)					
NRTL (α = 0.2)			1−2	−7894.0	7358.7
	F	0.4736	1−3	1031.3	13641
	$\Delta\beta$	6.70	2−3	4491.9	−659.82
[C$_8$mim][NTf$_2$] (1) + Pyridine (2) + *n*-Hexane (3)					
NRTL (α = 0.3)			1−2	−6343.1	4109.6
	F	0.5272	1−3	1608.8	11758
	$\Delta\beta$	8.4	2−3	3203.3	1187.6
[C$_2$mim][EtSO$_4$] (1) + Pyridine (2) + *n*-Hexane (3)					
NRTL (α = 0.3)			1−2	−20213	4537.4
	F	1.0814	1−3	9596.6	14532
	$\Delta\beta$	5.9	2−3	8247.3	−18003

Table 7. Binary Interaction Parameters and Root-Mean-Square Deviations (rmsd's) for the NRTL Correlation, Fixing the Solute-Distribution Ratio at Infinite Dilution, of the Ternary Systems at 298.15 K

			components	parameters	
model	rmsd		$i-j$	Δg_{ij}/J·mol^{-1}	Δg_{ji}/J·mol^{-1}
[C$_8$mim][BF$_4$] (1) + Pyridine (2) + *n*-Hexane (3)					
NRTL (α = 0.2)	F	0.5383	1−2	−6829.3	6065.8
	$\Delta\beta$	2.60	1−3	1183.0	16888
	β_∞	8.58	2−3	4841.3	−618.28
[C$_8$mim][NTf$_2$] (1) + Pyridine (2) + *n*-Hexane (3)					
NRTL (α = 0.3)	F	0.5789	1−2	−5326.9	3740.2
	$\Delta\beta$	5.5	1−3	1735.7	12808
	β_∞	10.53	2−3	3492.6	1484.8
[C$_2$mim][EtSO$_4$] (1) + Pyridine (2) + *n*-Hexane (3)					
NRTL (α = 0.3)	F	1.0744	1−2	−21005	4748.2
	$\Delta\beta$	5.8	1−3	9561.7	14850
	β_∞	2.75	2−3	8186.2	−18848

Table 8. Binary Interaction Parameters and Residuals for the Simultaneous Correlation of All Ternary Systems Involved in Gasoline-Synthetic Desulfurization Using the NRTL (α = 0.3) Equation at 298.15 K with [C_8mim][BF_4]

ternary system	NRTL (α = 0.3)	
	F	$\Delta\beta$
[C_8mim][BF_4] + thiophene + *n*-hexane	1.2924	5.5
[C_8mim][BF_4] + thiophene + *n*-heptane	1.7466	6.2
[C_8mim][BF_4] + thiophene + isooctane	1.7256	13
[C_8mim][BF_4] + thiophene + toluene	1.3784	5.1
[C_8mim][BF_4] + pyridine + *n*-hexane	1.1411	7.5

components		parameters	
i	j	$\Delta g_{ij}/\mathrm{J\cdot mol^{-1}}$	$\Delta g_{ij}/\mathrm{J\cdot mol^{-1}}$
[C_8mim][BF_4]	thiophene	−4951.5	14207
[C_8mim][BF_4]	*n*-hexane	3652.2	11918
thiophene	*n*-hexane	1127.9	505.94
[C_8mim][BF_4]	*n*-heptane	3739.3	12732
thiophene	*n*-heptane	406.88	−1129.9
[C_8mim][BF_4]	isooctane	4408	7398
thiophene	isooctane	5379.9	−1384.1
[C_8mim][BF_4]	toluene	−2302.2	11306
thiophene	toluene	−420.47	124.48
[C_8mim][BF_4]	pyridine	−3529	2744.5
pyridine	*n*-hexane	5147.3	755.33

Table 9. Binary Interaction Parameters and Residuals for the Simultaneous Correlation of All Ternary Systems Involved in Gasoline-Synthetic Desulfurization Using the NRTL (α = 0.3) Equation at 298.15 K with [C_8mim][NTf_2]

ternary system	NRTL (α = 0.3)	
	F	$\Delta\beta$
[C_8mim][NTf_2] + thiophene + *n*-hexane	4.7790	21.2
[C_8mim][NTf_2] + thiophene + *n*-heptane	3.4244	22.6
[C_8mim][NTf_2] + thiophene + isooctane	3.7548	39.5
[C_8mim][NTf_2] + thiophene + toluene	10.0927	15.1
[C_8mim][NTf_2] + pyridine + *n*-hexane	2.7869	10.8

components		parameters	
i	j	$\Delta g_{ij}/\mathrm{J\cdot mol^{-1}}$	$\Delta g_{ji}/\mathrm{J\cdot mol^{-1}}$
[C_8mim][NTf_2]	thiophene	−5103.2	17153
[C_8mim][NTf_2]	*n*-hexane	2876.2	12878
thiophene	*n*-hexane	2025.4	809.50
[C_8mim][NTf_2]	*n*-heptane	2947.8	10051
thiophene	*n*-heptane	2037.5	1365.0
[C_8mim][NTf_2]	isooctane	2790.6	11995
thiophene	isooctane	2583.4	1755.9
[C_8mim][NTf_2]	toluene	−2084.0	12986
thiophene	toluene	−71.427	−56.631
[C_8mim][NTf_2]	pyridine	−4281.2	1047.3
pyridine	*n*-hexane	3073.5	1603.3

Table 10. Binary Interaction Parameters and Residuals for the Simultaneous Correlation of All Ternary Systems Involved in Gasoline-Synthetic Desulfurization Using the NRTL (α = 0.3) Equation at 298.15 K with [C_2mim][$EtSO_4$]

ternary system	NRTL (α = 0.3)	
	F	$\Delta\beta$
[C_2mim][$EtSO_4$] + thiophene + *n*-hexane	1.6217	9.2
[C_2mim][$EtSO_4$] + thiophene + n-heptane	1.3301	10.1
[C_2mim][$EtSO_4$] + thiophene + isooctane	3.0131	20.3
[C_2mim][$EtSO_4$] + thiophene + toluene	1.1043	6.3
[C_2mim][$EtSO_4$] + pyridine + *n*-hexane	1.217	7.8

components		parameters	
i	j	$\Delta g_{ij}/\mathrm{J\cdot mol^{-1}}$	$\Delta g_{ji}/\mathrm{J\cdot mol^{-1}}$
[C_2mim][$EtSO_4$]	thiophene	−1930.3	10737
[C_2mim][$EtSO_4$]	*n*-hexane	10973	12940
thiophene	*n*-hexane	4055.8	−666.15
[C_2mim][$EtSO_4$]	*n*-heptane	12357	12925
thiophene	*n*-heptane	4992.5	−1035.3
[C_2mim][$EtSO_4$]	isooctane	11978	12682
thiophene	isooctane	4677.6	−2761.7
[C_2mim][$EtSO_4$]	toluene	2220.1	13981
thiophene	toluene	−207.51	573.84
[C_2mim][$EtSO_4$]	pyridine	−15305	4458.8
pyridine	*n*-hexane	7972.4	−12738

tion. Subscripts and superscripts are i for components of the mixture, j for phases (I, II), and k for tie-lines. Both functions include a penalty term (the second term) to reduce the risks of multiple solutions associated with parameters of high value, in which $Q = 10^{-6}$ for eq 3 and $Q = 10^{-10}$ for eq 4, and P_n are the adjustable parameters. F_b also includes a third term to correctly fit experimental results when working with low solute concentrations, in which $\hat{\gamma}^{\mathrm{I}}_{\mathrm{S}\infty}$ and $\hat{\gamma}^{\mathrm{II}}_{\mathrm{S}\infty}$ represent the solute activity coefficients calculated at infinite dilution in both phases and β_∞ is the solute molar distribution ratio at infinite dilution.

The quality of correlation is measured by the residual function F and the mean error of the solute distribution ratio, $\Delta\beta$:

$$F = 100\left[\sum_k \mathrm{mim} \sum_i \sum_j \frac{(x_{ijk} - \hat{x}_{ijk})^2}{6M}\right]^{0.5} \tag{5}$$

$$\Delta\beta = 100\left[\sum_k \frac{((\beta_k - \hat{\beta}_k)/\beta_k)^2}{M}\right]^{0.5} \tag{6}$$

where M refers to the number of experimental tie-lines.

In this work, experimental data were correlated in two ways: without defining an a priori value of β_∞, causing the last term of eq 2 to become zero, and specifying an optimal value of this parameter. An appropriate given value of β_∞ can improve the fit at low solute concentrations.

Table 6 shows the binary interaction parameters and residuals for the NRTL correlations of the ternary data without fixing an optimal value for the solute distribution ratio at infinite dilution. Table 7 shows the results of the correlations when an optimal value for the solute distribution ratio at infinite dilution was fixed at a value found by trial and error which minimizes $\Delta\beta$. In all of the cases, the value of the nonrandomness parameter which achieved best results was selected. Correlated compositions were included on Figures 2 to 4 for comparison with experimental values.

3.2. Simultaneous Correlation. By using the same correlation program previously cited, the simultaneous correlation of five ternary systems[3,4,7−11] involved in the gasoline and diesel desulfurization was carried out with the NRTL[12] equation without defining an a priori value of β_∞. Tables 8 to 10 show the binary interaction parameters and residuals for each ternary system when [C_8mim][BF_4], [C_8mim][NTf_2], and [C_2mim][$EtSO_4$] are, respectively, the ILs involved in desulfurization. The best results were achieved for a value of the nonrandomness parameter α = 0.3.

The simultaneous correlation of five ternary systems[6−11] involved in the diesel desulfurization was also carried out. Tables 11 to 13 show the binary interaction parameters and residuals for each ternary system when [C_8mim][BF_4], [C_8mim][NTf_2], and [C_2mim][$EtSO_4$] are, respectively, the ILs involved in desulfurization. As before, the best results were achieved for a value of the nonrandomness parameter α = 0.3.

4. Conclusions

LLE of several ternary systems involving *n*-hexane, pyridine, and [C_8mim][BF_4], [C_8mim][NTf_2], or [C_2mim]-

Table 11. Binary Interaction Parameters and Residuals for the Simultaneous Correlation of All Ternary Systems Involved in Diesel-Synthetic Desulfurization Using the NRTL (α = 0.3) Equation at 298.15 K with [C_8mim][BF_4]

ternary system	NRTL (α = 0.3) F	$\Delta\beta$
[C_8mim][BF_4] + thiophene + *n*-heptane	1.8974	5.5
[C_8mim][BF_4] + thiophene + *n*-dodecane	2.0049	7.0
[C_8mim][BF_4] + thiophene + *n*-hexadecane	2.7342	17.3
[C_8mim][BF_4] + thiophene + toluene	2.0802	4.2
[C_8mim][BF_4] + pyridine + *n*-hexane	1.1070	5.6

components i	j	parameters Δg_{ij}/J·mol^{-1}	Δg_{ji}/J·mol^{-1}
[C_8mim][BF_4]	thiophene	−3921.5	12762
[C_8mim][BF_4]	*n*-heptane	3680.3	12445
thiophene	*n*-heptane	813.77	264.63
[C_8mim][BF_4]	*n*-dodecane	5761.9	10601
thiophene	*n*-dodecane	1175.2	−2553.0
[C_8mim][BF_4]	*n*-hexadecane	7517.1	7182.1
thiophene	*n*-hexadecane	2547.5	−5437.9
[C_8mim][BF_4]	toluene	−2233.9	11325
thiophene	toluene	528.25	912.93
[C_8mim][BF_4]	*n*-hexane	3680.8	11200
[C_8mim][BF_4]	pyridine	−3680.6	2568.4
n-hexane	pyridine	693.21	5123.2

Table 12. Binary Interaction Parameters and Residuals for the Simultaneous Correlation of All Ternary Systems Involved in Diesel-Synthetic Desulfurization Using the NRTL (α = 0.3) Equation at 298.15 K with [C_8mim][NTf_2]

ternary system	NRTL (α = 0.3) F	$\Delta\beta$
[C_8mim][NTf_2] + thiophene + *n*-heptane	5.0283	18.6
[C_8mim][NTf_2] + thiophene + *n*-dodecane	4.8224	52.3
[C_8mim][NTf_2] + thiophene + *n*-hexadecane	6.7629	62.6
[C_8mim][NTf_2] + thiophene + toluene	10.9691	6.4
[C_8mim][NTf_2] + pyridine + *n*-hexane	3.8650	8.8

components i	j	parameters Δg_{ij}/J·mol^{-1}	Δg_{ji}/J·mol^{-1}
C_8mim][NTf_2]	thiophene	−4073.4	15288
[C_8mim][NTf_2]	*n*-heptane	2867.8	10547
thiophene	*n*-heptane	2325.4	1898.2
[C_8mim][NTf_2]	*n*-dodecane	4195.1	10982
thiophene	*n*-dodecane	2391.9	766.08
[C_8mim][NTf_2]	*n*-hexadecane	4824.1	8639.6
thiophene	*n*-hexadecane	1599.5	−142.22
[C_8mim][NTf_2]	toluene	−2034.6	13363
thiophene	toluene	134.10	127.60
[C_8mim][NTf_2]	*n*-hexane	3257.6	9580.0
[C_8mim][NTf_2]	pyridine	−5613.4	1359.7
n-hexane	pyridine	399.87	3094.0

Table 13. Binary Interaction Parameters and Residuals for the Simultaneous Correlation of All Ternary Systems Involved in Diesel-Synthetic Desulfurization Using the NRTL (α = 0.3) Equation at 298.15 K with [C_2mim][$EtSO_4$]

ternary system	NRTL (α = 0.3) F	$\Delta\beta$
[C_2mim][$EtSO_4$] + thiophene + *n*-heptane	1.8078	467.7
[C_2mim][$EtSO_4$] + thiophene + *n*-dodecane	3.7819	39.5
[C_2mim][$EtSO_4$] + thiophene + *n*-hexadecane	2.9146	33.3
[C_2mim][$EtSO_4$] + thiophene + toluene	1.5845	4.1
[C_2mim][$EtSO_4$] + pyridine + *n*-hexane	1.4023	9.0

components i	j	parameters Δg_{ij}/J·mol^{-1}	Δg_{ji}/J·mol^{-1}
[C_2mim][$EtSO_4$]	thiophene	−1426.2	9787.8
[C_2mim][$EtSO_4$]	*n*-heptane	10619	11182
thiophene	*n*-heptane	5414.2	−556.52
[C_2mim][$EtSO_4$]	*n*-dodecane	9701.4	12683
thiophene	*n*-dodecane	4912.7	−4539.1
[C_2mim][$EtSO_4$]	*n*-hexadecane	7350.9	12108
thiophene	*n*-hexadecane	5406.2	−6535.1
[C_2mim][$EtSO_4$]	toluene	1619.5	11856
thiophene	toluene	5195.2	−1756.0
[C_2mim][$EtSO_4$]	*n*-hexane	9631.5	11997
[C_2mim][$EtSO_4$]	pyridine	−11496	3465.5
n-hexane	pyridine	−9018.7	8507.4

[$EtSO_4$] ILs were obtained experimentally. Favorable values for the solute distribution ratio (β) were found for the three ILs, being in all cases higher than one. The [C_8mim][NTf_2] achieved higher values in this parameter, which implies a lower required amount of solvent to perform the extraction. High values for selectivities were also found for all of the studied ILs. Nonetheless, the more selective solvent was found to be the [C_2mim][$EtSO_4$] because of its low solubility in *n*-hexane. From a thermodynamic point of view, denitrogenation carried out by any of these ILs is feasible. The NRTL model has satisfactorily correlated the LLE experimental data of the studied systems. The best results were achieved for a value of the nonrandomness parameter α = 0.3.

With this researching work and some other previous papers, the ability of three ILs, [C_8mim][BF_4], [C_8mim][NTf_2], and [C_2mim][$EtSO_4$], to desulfurizate and denitrogenate fuel oils has been proved. The correlation of LLE experimental data is commonly desirable as it allows interpolation of tie-lines in the immiscible region of the system. Thus, equilibrium data can be easily managed for design purposes. The simultaneous correlation of the LLE data of the ternary systems involved in gasoline and diesel desulfurization was adequately carried out using the NRTL model.

Literature Cited

(1) Pagni, R. M., Ionic liquids as alternatives to traditional organic and inorganic solvents. In *Green Industrial Applications of Ionic Liquids*, 1st ed.; Rogers, R. D., Seddon, K. R., Volkov, S., Eds.; Kluwer Dordrecht: Netherlands, 2003; pp 105−128.

(2) Plechkova, N. V.; Seddon, K. R. Applications of ionic liquids in the chemical industry. *Chem. Soc. Rev.* **2008**, *37*, 123–150.

(3) Alonso, L.; Arce, A.; Francisco, M.; Rodríguez, O.; Soto, A. Liquid-Liquid Equilibria for systems composed by 1-methyl-3-octylimidazolium tetrafluoroborate ionic liquid, thiophene and *n*-hexane or cyclohexane. *J. Chem. Eng. Data* **2007**, *52*, 1729–1732.

(4) Alonso, L.; Arce, A.; Francisco, M.; Rodríguez, O.; Soto, A. Gasoline Desulfurization using Extraction with [C_8min][BF_4] Ionic Liquid. *AIChE J.* **2007**, *53*, 3108–3115.

(5) Alonso, L.; Arce, A.; Francisco, M.; Soto, A. Measurement and correlation of Liquid-Liquid Equilibria of two imidazolium ionic liquids with thiophene and methylcyclohexane. *J. Chem. Eng. Data* **2007**, *52*, 2409–2412.

(6) Alonso, L.; Arce, A.; Francisco, M.; Soto, A. (Liquid-Liquid) Equilibria of [C_8mim][NTf_2] ionic liquid with a sulfur-component and hydrocarbons. *J. Chem. Thermodyn.* **2008**, *40*, 265–270.

(7) Alonso, L.; Arce, A.; Francisco, M.; Soto, A. Phase behaviour of 1-methyl-3-octylimidazolium bis[trifluoromethylsulfonyl]imide with thiophene and aliphatic hydrocarbons: the influence of *n*-alkane chain length. *Fluid Phase Equilib.* **2008**, *263*, 176–181.

(8) Alonso, L.; Arce, A.; Francisco, M.; Soto, A. Solvent extraction of thiophene from n-alkanes (C_7, C_{12} and C_{16}) using the ionic liquid [C_8mim][BF_4]. *J. Chem. Thermodyn.* **2008**, *40*, 966–972.

(9) Alonso, L.; Arce, A.; Francisco, M.; Soto, A. Liquid-liquid Equilibria for [C_8mim][NTf_2] + Thiophene + 2,2,4-Trimethylpentane or + Toluene. *J. Chem. Eng. Data* **2008**, *53*, 1750–1755.

(10) Alonso, L.; Arce, A.; Francisco, M.; Soto, A. Liquid-Liquid equilibria of ([C_2mim][$EtSO_4$] + thiophene + 2,2,4 trimethylpentane) and ([C_2mim][$EtSO_4$] + thiophene + toluene): experimental data and correlation. *J. Solution Chem.* **2008**, *37*, 1355–1363.

(11) Alonso, L.; Arce, A.; Francisco, M.; Soto, A. Thiophene separation from aliphatic hydrocarbons using the 1-ethyl-3-methylimidazolium ethylsulfate ionic liquid. *Fluid Phase Equilib.* **2008**, *270*, 97–102.

(12) Renon, H.; Prausnitz, J. M. Local Compositions in Thermodynamic Excess Functions for Liquid Mixtures. *AIChE J.* **1975**, *21*, 116–118.

(13) Riddick, J. A.; Bunger, W. B.; Sakano, T. K. *Organic Solvents. Physical Properties and Methods of Purification*, 4th ed.; John Wiley & Sons: New York, 1986.

(14) Sanmamed, Y. A.; Gonzalez-Salgado, D.; Troncoso, J.; Cerdeirina, C. A.; Romani, L. Viscosity-induced errors in the density determination of room temperature ionic liquids using vibrating tube densitometry. *Fluid Phase Equilib.* **2007**, *252*, 96–102.

(15) Przybysz, K.; Drzewinska, E.; Stanislawska, A.; Wysocka-Robak, A.; Cieniecka-Roslonkiewicz, A.; Foksowicz-Flaczyk, J.; Pernak, J. Ionic Liquids and Paper. *Ind. Eng. Chem. Res.* **2005**, *44*, 4599–4604.

(16) Papaiconomou, N.; Yakelis, N.; Salminen, J.; Bergman, R.; Prausnitz, J. M. Synthesis and Properties of Seven Ionic Liquids Containing 1-Methyl-3-octylimidazolium or 1-Butyl-4-methylpyridinium Cations. *J. Chem. Eng. Data* **2006**, *51*, 1389–1393.

(17) Gómez, E.; González, B.; Calvar, N.; Tojo, E.; Domínguez, A. Physical Properties of Pure 1-Ethyl-3-methylimidazolium Ethylsulfate and Its Binary Mixtures with Ethanol and Water at Several Temperatures. *J. Chem. Eng. Data* **2006**, *51*, 2096–2102.

(18) Sørensen, J. M.; Arlt, W. *Liquid-Liquid Equilibrium Data Collection*; DECHEMA Chemistry Data Series: Frankfurt, 1980.

Received for review January 22, 2010. Accepted March 21, 2010. The authors are thankful for financial support under project CTQ2009-10776 from the Ministerio de Educación y Ciencia (Spain).

JE100075M